Published in final edited form as:
Angew Chem Int Ed Engl. 2011 April 26; 50(18): 4161–4164. doi:10.1002/anie.201100115.

Micromachine Enabled Capture and Isolation of Cancer Cells in Complex Media

Shankar Balasubramanian[§], **Daniel Kagan**[§], **Che-Ming Jack Hu**, **Susana Campuzano**, **M. Jesus Lobo-Castañon**, **Nicole Lim**, **Dae Y. Kang**, **Maria Zimmerman**, **Liangfang Zhang**[*], and **Joseph Wang**[*]
Department of NanoEngineering, University of California - San Diego, La Jolla, CA 92093 USA, Fax: (+1) 858-534-9553

Circulating tumor cells (CTCs) are the primary entities responsible for spawning cancer metastasis. Detection of CTCs provides an indicator for the clinical diagnosis and prognosis of various types of cancers. Several approaches, based primarily on flowing the sample through antibody-coated magnetic-beads[1] or microchip[2,3] surfaces have been described for isolating and counting CTCs. However, these approaches require extensive sample preparation and/or complex surface microstructures to detect the extremely low abundance of CTCs in blood.[3,4] In this study we describe a immunomicromachine-based approach for an in-vitro isolation of cancer cells that holds promise for direct CTC detection without sample pre-processing.

Recent progress in the field of man-made nanomachines,[5] particularly major advances in the power, efficiency, motion control and versatility of artificial nanomotors,[6] have opened the door to new and important biomedical applications, ranging from drug delivery[7] to biosensing.[8] Autonomously moving synthetic nanomotors have recently been employed for the pickup and transport of diverse payloads, mostly via magnetic or electrostatic interactions.[9] Extending the scope of chemically-powered nanomotors to physiological conditions represents a key challenge since such nanomotors are commonly incompatible with the high ionic strength environment of biological fluids. Catalytic rolled-up microtube rockets, propelled by the recoiling force of accumulated gas bubbles,[6a,9d,e,10] are particularly attractive for isolating and transporting cancer cells for downstream analysis as they possess the necessary towing force to carry large mammalian cells. Here we demonstrate that these microrockets overcome previous constraints to locomotion in biological fluids and are readily functionalized with an antibody specific for antigenic surface proteins expressed on cancer cells, such as anti-carcinoembryonic antigen (anti-CEA) monoclonal antibody (mAb).[11] CEA is used as a targeting antigen because it is one of the most common antigens among cancer cells, being over-expressed in approximately 95% of colorectal, gastric and pancreatic cancers.[12] Figure 1 conceptually illustrates the microrockets based pick-up and transport of cancer cells. The conjugation of the anti-CEA mAb to the outer gold surface of the microrockets is accomplished through carboxyl-terminated groups from a binary self-assembled monolayer (SAM) using standard EDC/NHS chemistry (see inset in Figure 1 and Experimental Section for details).

Practical cancer cell sorting applications require that effective motor propulsion is maintained in relevant physiological fluids. For example, Figure 2 and the corresponding

[*]josephwang@ucsd.edu, zhang@ucsd.edu.
[§]These authors contributed equally to this work.

Supporting information for this article is available on the WWW under http://www.angewandte.org or from the author.

Supporting Information Video 1 illustrate the movement of the mAb-coated microrocket in human serum (diluted 1:4 to include the microrockets and fuel). These images show a long tail of microbubbles, catalytically generated on the inner platinum surface and released from the rear of the microtube. Such ejection of bubbles propels the microrocket in the diluted serum medium at a relatively high speed of about 85 μm/s. The sandwiched ferromagnetic (Fe) layer of the microrocket (see Experimental Section) offers convenient guidance of the microrocket via tuning of the external magnetic-field direction. To facilitate effective propulsion and navigation in such biological media (even after the surface functionalization) the thickness of the Fe layer was increased at least 3 times compared to previously described microrockets.[6a,9d,10a]

These mAb-functionalized microrockets can selectively bind to target cancer cells and then effectively transport them in PBS and serum. For example, the time-lapse images of Figure 3 along with the corresponding video clips (Supporting Information Video 2), display the pickup of a CEA+ pancreatic cancer cell by the anti-CEA mAb-modified microrocket in PBS (a) and diluted human serum (b). These images and videos demonstrate the movement of the microrocket towards the CEA+ cell (top panel), the dynamic 'en route' capture of the cell (middle panel), and subsequent directed travel of the cancer-cell loaded micromotor over a pre-selected path (bottom panel) without compromising the trajectory of the microrocket movement. Notice that the high speed of the microrocket is only slightly affected by the cell loading (e.g., decreasing from 85 to 80 μm/s in serum environment), reflecting its high towing force. Such successful pick-up is observed nearly 80% (n = 43) of the time during the first interaction between the modified microrockets and the CEA+ cells while the efficiency decreases to 70% in serum. Note that the cells were not observed to non-specifically bind to the microrocket during the various control experiments (see below) except in the case when they were sucked up into the microrocket's opening (representing 2% of the time, n = 120).

The substantial force essential for transporting a relatively large (~16 μm) cancer cell reflects the bubble recoiling propulsion mechanism of the microrockets. The velocity-dependent drag force of the microrockets has been estimated from Stokes' law (see Supporting Information for detailed analysis). The minimum force necessary for transporting such large cells at 1 body-length/sec is 2.5 pN (See Supporting Information Table S1), which is an order of magnitude larger than the force generated by previously developed magnetically or chemically-powered nano/microscale motors.[7,13]

Unmodified microrockets usually move at a high speed of up to 2 mm/s in PBS media (not shown), thus exerting a force up to 250 pN. However, after the surface modification with the antibody these microrockets travel in the same bulk media at a speed of up to 150 μm/s, thus generating an estimated force of ~18 pN. Partial blocking by adsorbed proteins and sulfur poisoning of catalytic platinum surface[14] may account for this diminished speed. In the presence of diluted serum, the maximum microrocket speed in the bulk solution further drops to ~100 μm/s, reflecting the increased solution viscosity. Even at the lower speed, the microrockets have sufficient force (> 13 pN) to overcome the additional drag force due to the capture of a cancer cell and are demonstrated to transport the cell over long periods (> 60 s; see Supporting Information Video 3 for a shorter time period and distance). The lower microrocket speed is actually advantageous for the cell capture and transport, as it reduces the shear stress and allows for sufficient antigen/antibody interaction. The upper limit of the microrocket speeds in PBS and serum result in estimated shear stresses of 2.3 and 1.7 dyn/cm^2, respectively (See Supporting Information Table S2). Such values have been commonly observed when selectively capturing flowing cells via antibody interaction in microfluidic devices.[2, 15]

The specific binding of CEA+ cancer cells to anti-CEA mAb-modified microrockets was verified by control experiments. These experiments involved the interactions between anti-CEA mAb- modified microrockets and CEA− pancreatic cancer cells and between SAM-modified microrockets without the mAb and CEA+ pancreatic cancer cells (Figure 4 and Supporting InformationVideo 4; see Experimental Section for preparation of these 'control' microrockets). The results illustrate that none of the controls have the capability of picking up cancer cells (Figure 4c–h). Only the anti-CEA mAb-modified microrockets are able to capture the target CEA+ cancer cells (Figure 4a,b). For these control experiments, we deliberately selected microrockets that moved slower along the glass slide interface (average speed of 45 μm/s) as a way to minimize the exerting shear stress (0.7 dynes/cm^2, see Supporting Information Table S2) and maximize the microrocket/cell interaction time. We further confirmed that the interaction between the CEA+ cell and mAb-modified microrocket was strong and specific by oscillating the pair vigorously using a magnet (Supporting Information Video 5). These results, along with the subsequent studies involving cells mixture (CEA+ and CEA− cells; shown below) clearly demonstrate that the capture of the cancer cell occurs through the specific antigen recognition.

The viability of the cells under the conditions used in the present study was examined using the trypan blue exclusion assay (See Supporting Information Table S3 and Figure S2). The cancer cells were subject to PBS solutions containing various levels of the peroxide fuel. While over half of the cells remained viable for over 10 minutes at the 8% peroxide level, the majority of the cells (>90%) remained viable after 1 hour immersion in a 2% peroxide solution. Such time windows would allow for the retrieval of cells for subsequent analysis. It is important to note that we also observed the ability of the mAb-coated microrockets to bind to dead CEA+ cells or their cellular membrane fragments. Therefore, from a cellular detection perspective, these microrockets can identify any CEA expressing cell regardless of its viability.

The ability of the anti-CEA mAb-modified microrockets to identify and isolate target cancer cells was further demonstrated using a mixture of green fluorescently stained CEA+ and unstained CEA− cancer cells. As shown in the overlay images of Figure 5 (taken from Supporting Information Video 6), the microrocket first closely interacts with the CEA− cell (steps 1–2), hitting and displacing it to a different focal plane (due to lack of reaction). After such direct contact without pickup of the CEA− cell, the microrocket captures and transports a CEA+ cell (steps 4–5). Note (from the video) that the CEA+ cell is tightly bound to the modified microrocket during deliberate oscillations. This selective binding was confirmed by exposing the sample to a blue light (460 nm), which excites the CEA+ cells stained with a green fluorescent dye (step 5). The CEA− cells are indicated by a lack of fluorescence while exposed to blue light at the beginning of the video. A microrocket moving along the bottom plane was chosen because its reduced speed allows us to properly guide the microrocket and distinguish the fluorescent CEA+ cells (from CEA− cells on the same plane) under the necessary magnification (40x). A similar experiment involving the incubation of modified microrockets (without fuel) with a mixture of CEA+ and CEA-cells further demonstrates the selectivity of the mAb-modified microrocket (Supporting Information Figure S3). These experiments confirm the ability of microrockets to selectively recognize target cancer cells in cell mixtures.

In conclusion, we have demonstrated a new in-vitro strategy for isolating cancer cells based on the selective binding and transport ability of mAb-functionalized microengine rockets. These microrockets can be readily functionalized with targeting ligands such as mAb for highly specific cancer cell selection and provide sufficient propulsive force for the efficient transport of the captured target cells in biological fluids. While the concept has been illustrated for the capture of pancreatic cancer cells, it could be expanded to other cancer cell

lines. Such microrocket-based selective capture and transport of tumour cells without pre-processing biological samples holds great promise for extracting CTCs from biological fluids and hence for the early diagnosis of cancer and its recurrence. The autonomous transport properties of the microrockets in viscous fluids such as serum might eliminate multiple preparatory steps involved in the existing magnetic bead-based systems.[2] In addition, the ability to alter the nature of interactions (by controlling the shear stress) could increase the efficiency of the viable cell separation process. This micromachine-based cell manipulator and sorter could be readily incorporated in microchannel networks for creating integrated microchip devices. Such microchips will rely on the active transport of multiple immunomicromachines in a blood sample reservoir to induce numerous interactions, high capture efficiency and single-step isolation of CTCs. Furthermore, this can be extended to accumulating CTCs in a predefined ‘collection’ area by detaching the captured cells.

Supplementary Material

Refer to Web version on PubMed Central for supplementary material.

Acknowledgments

This work was supported by the National Science Foundation (Award Number CBET 0853375 to JW) and by the National Institute of Health (Grant Number U54CA119335 to LZ). M.J.L.C thanks the University of Oviedo and the Spanish MICINN (PR 2009-0430). The authors thank M. Benchimol, B. Chuluun and Prof. S. Esener for their help.

References

1. Galanzha EI, Shashkov EV, Kelly T, Kim JW, Yang L, Zharov VP. Nature Nanotech. 2009; 4:855–860.
2. Nagrath S, et al. Nature. 2007; 450:1235–1239. [PubMed: 18097410]
3. Adams AA, et al. J Am Chem Soc. 2008; 130:8633–8641. [PubMed: 18557614]
4. Allan AL, Keeney M. J Oncol. 2010:426218 . [PubMed: 20049168]
5. a) Mirkovic T, Zacharia NS, Scholes GD, Ozin GA. ACS Nano. 2010; 4:1782–1789. [PubMed: 20420469] b) Wang J. ACS Nano. 2009; 3:4–9. [PubMed: 19206241] c) Mallouk TE, Sen A. Sci Amer. 2009; 300:72–77. [PubMed: 19438052]
6. a) Solovev AA, Mei YF, Bermúdez Ureña E, Huang GS, Schmidt OG. Small. 2009; 5:1688–1692. [PubMed: 19373828] b) Wang J, Manesh KM. Small. 2010; 6:338–345. [PubMed: 20013944] c) Paxton WF, Sundararajan S, Mallouk TE, Sen A. Angew Chemie Int Ed. 2006; 45:5420–5429.d) Ebbens SJ, Howse JR. Soft Matter. 2010; 6:726–738.
7. Kagan D, et al. Small. 2010; 6:2741–2747. [PubMed: 20979242]
8. Wu J, Balasubramanian S, Kagan D, Manesh KM, Campuzano S, Wang J. Nature Commun. 2010; 1:36.10.1038/ncomms1035 [PubMed: 20975708]
9. a) Sundararajan S, Lammert PE, Zudans AW, Crespi VH, Sen A. Nano Letters. 2008; 8:1271–1276. [PubMed: 18416540] b) Burdick J, Laocharoensuk R, Wheat PM, Posner JD, Wang J. J Am Chem Soc. 2008; 130:8164–8165. [PubMed: 18533716] c) Sundarajan S, Sengupta S, Ibele ME, Sen A. Small. 2010; 6:1479–1482. [PubMed: 20564727] d) Solovev AA, Sanchez S, Pumera M, Mei YF, Schmidt OG. Adv Func Mater. 2010; 20:2430–2435.e) Sánchez S, Solovev AA, Schulze S, Schmidt OG. Chem Commun. 2011; 47:698–700.
10. a) Mei Y, et al. Adv Mater. 2008; 20:4085–4090.b) Manesh KM, Cardona M, Yuan R, Clark M, Kagan D, Balasubramanian S, Wang J. ACS Nano. 2010; 4:1799–1804. [PubMed: 20230041]
11. Shi ZR, Tacha D, Itzkowitz SH. J Histochem Cytochem. 1994; 42:1215–1219. [PubMed: 7520463]
12. Zieglschmid V, Hollmann C, Böcher O. Crit Rev Clin Lab Sci. 2005; 42:155–196. [PubMed: 15941083]
13. Zhang L, Abbott JJ, Dong L, Peyer KE, Kratochvil BE, Zhang H, Bergeles C, Nelson BJ. Nano Lett. 2009; 9:3663–3667. [PubMed: 19824709]

14. Bartholomew, CH.; Agrawal, PK.; Katzer, JR. Advances in Catalysis. Vol. 31. Academic Press, Inc; 1982. p. 135-242.

15. Plouffe BD, Kniazeva T, Mayer JE Jr, Murthy SK, Sales VL. FASEB J. 2009; 23:3309–3314. [PubMed: 19487310]

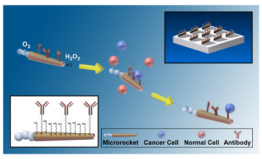

Figure 1.

Microrockets for capture and isolation of cancer cells. Upon encountering the cells, the anti-CEA mAb-modified microrockets recognize the CEA surface antigens on the target cancer cells, allowing their selective pick-up and transport. The top-right and bottom-left insets illustrate the preparation of the Ab-modified microrockets and the surface chemistry used for such functionalization, respectively.

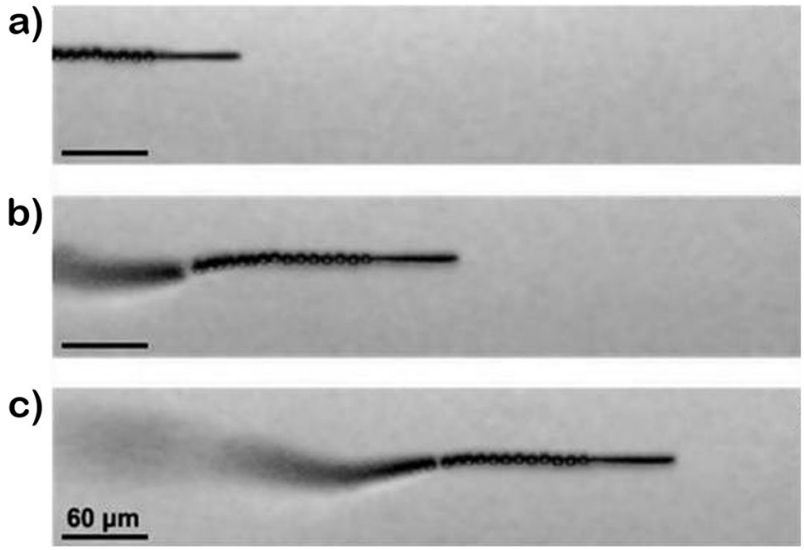

Figure 2.

Motion in human serum. Time-lapse images, taken from Video 1, showing the motion of an anti-CEA mAb-coated microrocket in human serum at 2 s intervals (a–c). Conditions, diluted human serum containing 7.5% (w/v) H_2O_2 and 1% (w/v) sodium cholate.

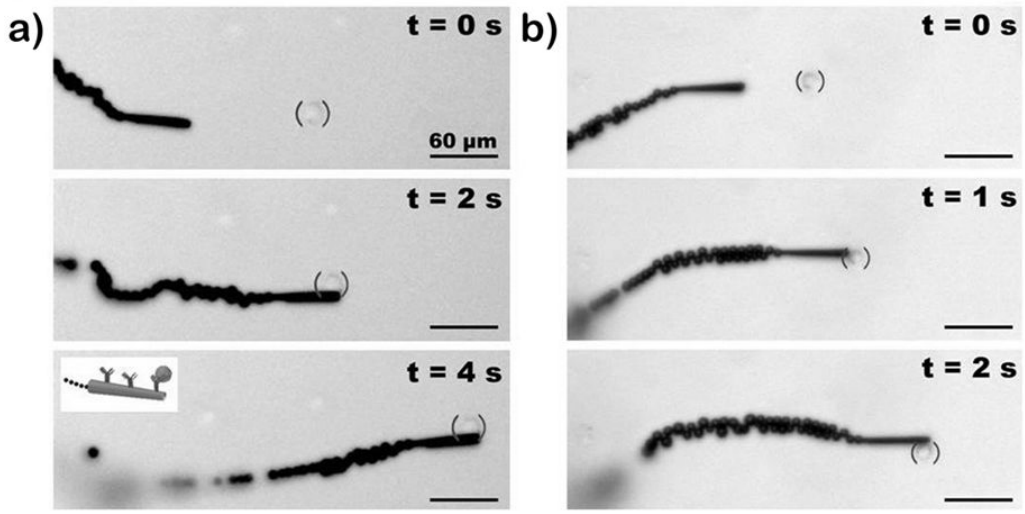

Figure 3.

Pick up and transport in PBS and diluted serum. Time-lapse images – taken from Video 2 – demonstrating the pickup and transport of a CEA+ pancreatic cancer cell by an anti-CEA mAb-modified microrocket in PBS (a) and human serum (b) at 2 s and 1 s intervals, respectively. Conditions, 1×PBS buffer (pH 7.4) (a) and diluted human serum (b), containing 7.5% (w/v) H_2O_2 and 1% (w/v) sodium cholate. CEA+ cells were accented using solid parenthesis.

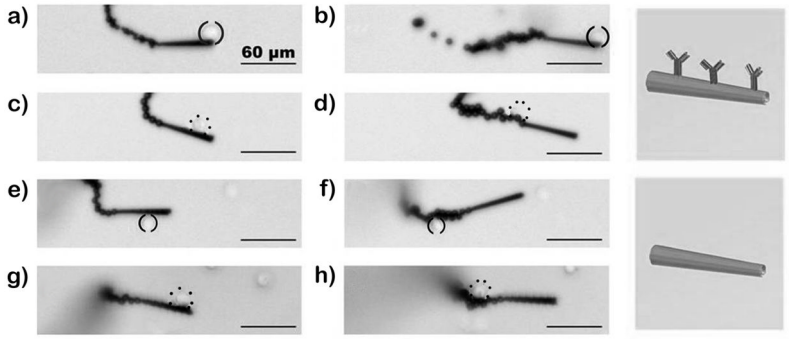

Figure 4.

Selectivity. Time-lapse images – taken from Video 4 – during (left) and after (right) the interaction between anti-CEA mAb-modified (ad) and unmodified (e–h) microrockets with CEA+ (a,b,e and f; solid parenthesis) and CEA− cancer cells (c,d,g and h; dotted parenthesis). Conditions,, as in Figure 3a.

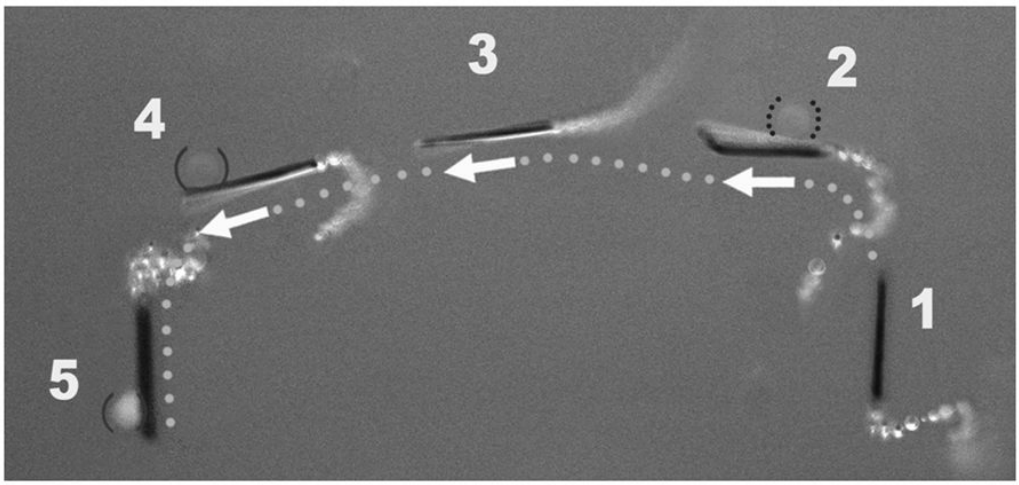

Figure 5.
Isolation of a CEA+ cell in mixture of cells. Overlay images taken from Supporting Information Video 6 – showing sequential steps (1–5) of movement of the anti-CEA mAb-modified microrocket in a mixture of CEA+ and CEA− cells (solid and dotted parenthesis, respectively). For clear visualization, step 5 has been slightly displaced. Conditions, as in Figure 4.